Supramolecular Triblock Copolymers Containing Complementary Nucleobase Molecular Recognition

Brian D. Mather,[†] Margaux B. Baker,[†] Frederick L. Beyer,[‡] Michael A. G. Berg,[†] Matthew D. Green,[†] and Timothy E. Long[†,*]

Macromolecules and Interfaces Institute, Department of Chemistry, Virginia Polytechnic Institute and State University, Blacksburg, Virginia 24061-0344, and Army Research Laboratory, Materials Division, Aberdeen Proving Ground, Aberdeen, Maryland 21005

Received April 12, 2007; Revised Manuscript Received July 9, 2007

ABSTRACT: A novel difunctional alkoxyamine initiator, $DEPN_2$, was synthesized and utilized as an efficient initiator in nitroxide-mediated controlled radical polymerization of triblock copolymers. Complementary hydrogen-bonding triblock copolymers containing adenine (A) and thymine (T) nucleobase-functionalized outer blocks were synthesized. These thermoplastic elastomeric block copolymers contained short nucleobase-functionalized outer blocks ($M_n \sim$ 1K−4K) and *n*-butyl acrylate rubber blocks of variable length ($M_n \sim$ 14K−70K). Hydrogen-bonding interactions were observed for blends of the complementary nucleobase-functionalized block copolymers in terms of increased specific viscosity as well as higher scaling exponents for specific viscosity as a function of solution concentration. In the solid state, the blends exhibited evidence of a complementary A−T hard phase, which formed upon annealing, and dynamic mechanical analysis (DMA) revealed higher softening temperatures. Morphological development of the block copolymers was studied using SAXS and AFM, which revealed intermediate interdomain spacings and surface textures for the blends compared to the individual precursors. Hydrogen-bonding interactions enabled the compatibilization of complementary hydrogen-bonding guest molecules such as 9-octyladenine.

Introduction

Hydrogen-bonding enables the introduction of thermoreversible properties into macromolecules through the creation of specific noncovalent intermolecular interactions.[1] Recent interest in hydrogen bonding in both supramolecular[2] and macromolecular[3] design has inspired numerous new explorations. The strength of these interactions is highly dependent on temperature,[4] solvent,[5] humidity,[6] and pH,[7] thus allowing control of properties through a number of environmental parameters. The resulting polymers often exhibit a stronger temperature dependence of melt viscosity than non-hydrogen-bonding polymers, suggesting possible advantages in melt processing.[8] The strength of hydrogen-bonding associations is further tunable via structural and geometric parameters as well as molecular design of the hydrogen-bonding sites.[9−13] Association strengths range from 10^2 M^{-1} for DNA nucleobases,[14] to self-complementary ureidopyrimidone (UPy) hydrogen-bonding groups,[2,15] which possess association constants on the order of 10^7 M^{-1}.

Sivakova and Rowan recently reviewed the use of nucleobases in supramolecular assembly and hydrogen-bonding polymers.[16] Rowan et al. noted that the behavior of the isolated nucleobases in synthetic polymers is quite different from their behavior in DNA where they are bound to a complementary base.[17] Multiple complementary association modes are possible for nucleobases, including the classical Watson−Crick mode[16] which is present in DNA as well as the less-commonly observed Hoogsteen association mode.[18] Furthermore, nucleobases exhibit several weak self-association modes (K_a < 10 M^{-1}),[14] which compete with the complementary association modes.

Hydrogen-bonding block copolymers differ from randomly functionalized copolymers since the placement of the hydrogen-bonding groups is localized to a specific region of the polymer backbone. This leads to a dramatic difference in morphology and physical properties due to a potential synergy between microphase separation and hydrogen-bonding interactions. Multiplicative and cooperative effects of the neighboring hydrogen-bonding groups lead to stronger associations[19,20] which reinforce microphase separation. Wilkes and co-workers have shown that single-urea-containing hard segments enable the development of filamentous hard phases.[21] Therefore, only short hydrogen-bonding blocks are necessary to achieve microphase separation.[22] In some cases, microphase separation can occur even for a single hydrogen-bonding group at the chain ends (i.e., telechelic functionality).[17] Others have noted the synergy between microphase separation and hydrogen bonding.[2] Furthermore, specific hydrogen-bonding interactions increase the effective Flory−Huggins binary segmental interaction parameter (χ) due to increased solubility parameter differences between the two blocks.[23] Nowick et al. also observed enhanced hydrogen-bonding interactions through localization of nucleobases in sodium dodecyl sulfate micellar cores in aqueous media.[24]

Others have previously synthesized nucleobase-containing block copolymers via living polymerization techniques such as atom transfer radical polymerization (ATRP)[25−30] and ring opening methathesis polymerization (ROMP).[31,32] Van Hest et al. synthesized thymine-functionalized block copolymers via ATRP of a thymine methacrylate monomer from a PEG-macroinitiator.[25] Thymine-containing, cinnamate-functionalized photo-cross-linkable block copolymers were synthesized via ATRP.[26−30] Hydrogen-bonding interactions facilitated association of guest molecules into the core of micelles which were formed in selective solvents. The micelles were then photo-cross-linked and the hydrogen-bonding guest molecules were

* Corresponding author. E-mail: telong@vt.edu. Telephone: (540) 231-2480. Fax: (540) 231-8517.

[†] Macromolecules and Interfaces Institute, Department of Chemistry, Virginia Polytechnic Institute and State University.

[‡] Army Research Laboratory, Materials Division, Aberdeen Proving Ground.

10.1021/ma070865y CCC: $37.00
Published on Web 08/28/2007

Scheme 1. (a) Synthesis of Adenine and Thymine Nucleobase-Functionalized Triblock Copolymers and (b) Pictorial Representation of the Hydrogen Bonding Association of Complementary Adenine and Thymine Block Copolymers in Polymer Blends

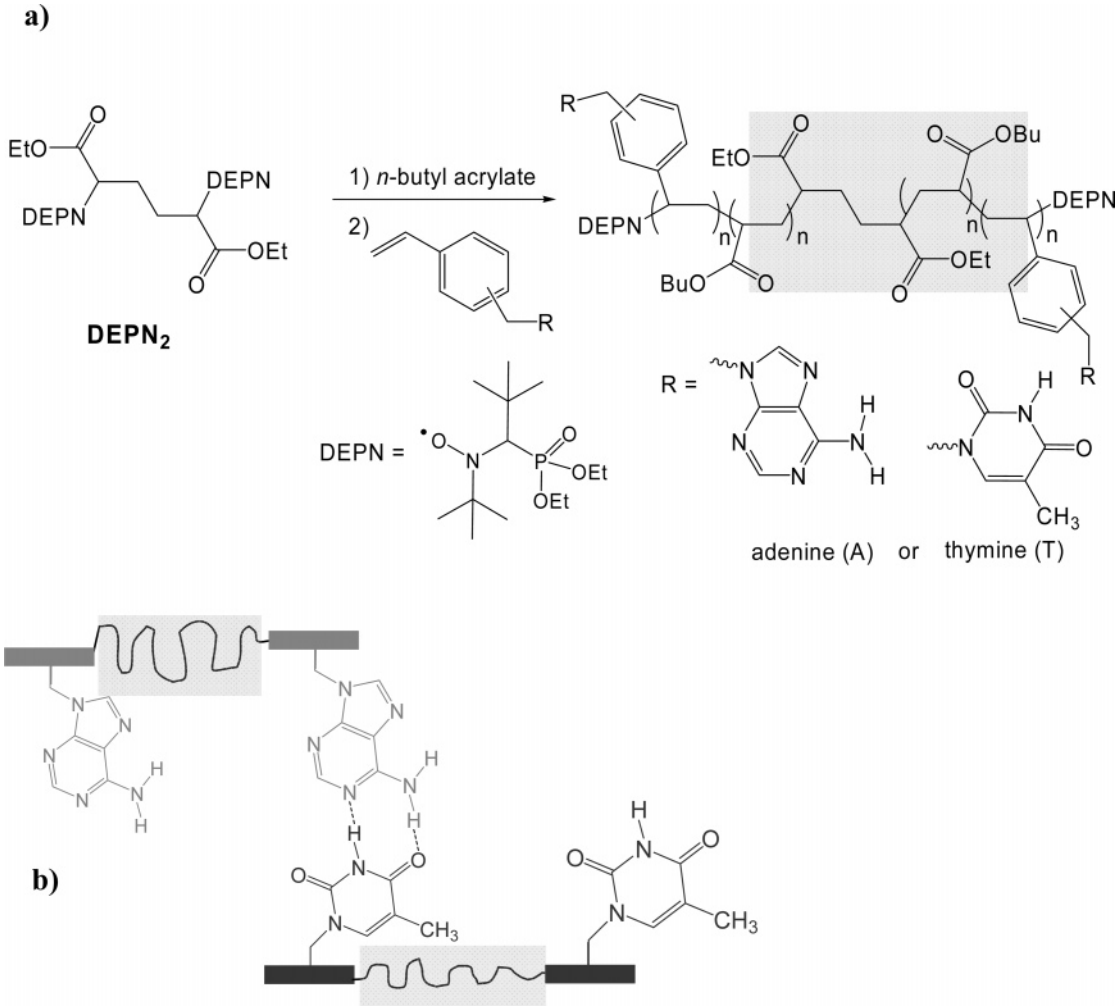

extracted, resulting in hollow nanospheres for potential drug delivery applications. Sleiman et al. have synthesized adenine-functionalized block copolymers through ROMP of substituted oxonorbornene monomers, and subsequently formed cylindrical-shaped structures during evaporation from dilute solution.[31] Weck et al. recently demonstrated the combination of nucleobase hydrogen-bonding and metal−ligand coordination interactions in block copolymers synthesized via ROMP.[32] Matsushita et al. have also synthesized nucleoside-containing block copolymers using stepwise phosphoramidite coupling techniques.[33] Significant effort was also devoted to studying nucleobase-containing homopolymers and random polymers.[3,4,34−39]

Nitroxide mediated polymerization (NMP) is a well-established controlled radical polymerization methodology which enables block copolymer synthesis with a wide range of acrylic and styrenic monomers.[40] Controlled radical polymerization techniques are particularly suited for the hydrogen-bonding block copolymers, due to tolerance for protic functionality[40] and absence of residual catalyst metals, which were demonstrated to coordinate to nucleobases and affect polymerization kinetics.[25] Despite the many advantages of nitroxide-mediated polymerization, only one brief report exists in the prior literature regarding synthesis of nucleobase-functionalized block copolymers using NMP.[41] In the present work, *N*-*tert*-butyl-*N*-(1-diethylphosphono-2,2-dimethylpropyl)-*N*-oxyl (DEPN, Scheme 1) nitroxide is utilized, which was developed earlier by Gnanou and Tordo, and is capable of mediating the polymerization of acrylic monomers.[42] In order to achieve symmetric triblock copolymers in two synthetic steps, a novel difunctional alkoxyamine initiator ($DEPN_2$, Scheme 1) was utilized in the present polymerizations. The use of difunctional initiation is further advantageous due to the difficulties in crossover from styrenic to acrylic monomers that are observed in nitroxide mediated polymerization.[43] Furthermore, alkoxyamine initiators facilitate controlled molecular weights due to the 1:1 stoichiometry between the initiating fragment and the nitroxide and allow chain-end functionality as reported earlier in our laboratories.[44,45]

In this manuscript, we discuss combinations of nitroxide-mediated radical polymerization with complementary adenine (A) and thymine (T) nucleobase hydrogen bonding in block copolymer architectures (Scheme 1). Furthermore, we examine the effects of hydrogen bonding in blends of complementary nucleobase-functionalized block copolymers. Because of the atactic polymer backbone in the present work, a well-ordered double helical complex is not predicted as suggested from the structure of DNA. Instead, associated structures are more likely to consist of multiple polymer chains with one or more associated A-T nucleobase pairs. Future work will involve substitution on tactic polymers to ascertain the influence of tacticity on the strength of the assocations.

Experimental Section

Materials. *n*-Butyl acrylate (99%) was purchased from Aldrich and purified using an alumina column and subsequent vacuum

distillation from calcium hydride. Diethyl-*meso*-2,5-dibromoadipate (98%), copper(I) bromide (99.999%), *N*,*N*,*N*′,*N*″,*N*″-pentamethyldiethylenetriamine (PMDETA) (98%) and *N*,*N*-dimethylformamide (DMF, anhydrous, 99.8%) were purchased from Aldrich and used without further purification. Copper powder (45 μm, 99%) was purchased from Acros and used as received. DEPN,[42] styryl-DEPN,[46] 1-vinylbenzyl thymine,[47] 9-vinylbenzyladenine,[48] and 9-octyladenine[49] were synthesized according to the previous literature.

Synthesis of $DEPN_2$. DEPN (2.0 g, 6.8 mmol) and diethyl-*meso*-2,5-dibromoadipate (1.36 g, 3.8 mmol) were charged to a one-necked 100 mL round-bottomed flask containing a magnetic stirbar. CH_2Cl_2 (30 mL) was added and the solution was degassed with three freeze−pump−thaw cycles. In a second 100 mL round-bottomed flask, PMDETA (2.34 g, 13.6 mmol) was dissolved in 20 mL CH_2Cl_2 and subjected to the same degassing. In a third 100 mL round-bottomed flask containing a stirbar, CuBr (0.78 g, 5.47 mmol) and Cu powder (0.35 g, 5.47 mmol) were purged with nitrogen gas. After degassing, the liquid reagents were transferred using a cannula into the flask containing the copper powder and CuBr. The reaction was stirred at 25 °C for 24 h, diluted with CH_2Cl_2 (200 mL), and washed repeatedly with water (10 × 100 mL), to remove copper compounds. The organic layer was then dried over sodium sulfate and evaporated. The product was separated on silica, eluting with ethyl acetate:hexane (1:1). The difunctional alkoxyamine initiator based on DEPN nitroxide ($DEPN_2$,as shown in Scheme 1) was isolated as a mixture of diastereomers. FAB MS: m/z = 789.4842 $[M + H]^+$ experimental, m/z = 789.48 theoretical. A peak for the monofunctional product was not observed (m/z = 574.5). ^{1}H NMR (400 MHz, $CDCl_3$,25 °C) (δ, ppm): 1.0−1.2 ppm (s, tBu, 36H), 1.2−1.4 ppm (m, ester CH_3, 18H), 1.6−2.4 ppm (br s, linker CH_2, 4H), 3.1−3.6 ppm (m, DEPN CH, 2H), 3.9−4.2 ppm (m, CH_3, 12H), 4.4−4.5 ppm (m, COC*H*, 2H). ^{13}C NMR (101 MHz, $CDCl_3$, 25 °C) (δ, ppm): 13.90, 13.98, 14.03, 16.08, 16.14, 16.32, 16.35, 16.41, 16.47, 26.46, 26.52, 26.67, 26.96, 27.53, 27.56, 27.89, 27.95, 28.12, 29.38, 29.44, 29.89, 29.93, 30.12, 30.18, 34.48, 35.09, 35.16, 35.21, 35.49, 35.58, 35.64, 58.82, 58.89, 60.22, 60.27, 60.32, 60.40, 60.62, 61.57, 61.66, 61.96, 62.03, 62.23, 62.30, 68.62, 68.90, 69.99, 70.27, 75.31, 76.85, 77.20, 81.52, 81.87, 86.31, 86.74, 171.46, 172.74. ^{31}P NMR (162 MHz, $CDCl_3$, 25 °C) (δ, ppm): 24.91, 25.00, 25.20, 25.59, 25.63, 25.82.

***meso*-Diastereomer of $DEPN_2$:** The *meso* diastereomer was isolated from the partly crystalline fractions, which eluted first during chromatographic purification of $DEPN_2$. Further separation was achieved via triturating the semicrystalline mixture with hexane. Mp = 139.5−141.5 °C. ^{1}H NMR (400 MHz, $CDCl_3$, 25 °C) (δ, ppm): 1.03 (s, *N*-tBu, 18H), 1.06 (s, *C*-tBu, 18H), 1.24 (m, ester CH_3, 18H), 1.55−2.40 (br, linker CH_2, 4H), 3.18 (d, J = 25 Hz, DEPN CH, 2H), 3.85−4.20 (m, OCH_2, 12H), 4.25−4.46 (br, OCH, 2H). ^{13}C NMR (101 MHz, $CDCl_3$, 25 °C) (δ, ppm): 13.95, 16.31 (dd, J_1 = 28.4 Hz, J_2 = 6.2 Hz), 27.94, 28.57, 29.31 (d, J = 6.2 Hz), 35.59 (d, J = 5.4 Hz), 58.69 (d, J = 7 Hz), 61.05 (d, J = 95 Hz), 61.80 (d, J = 6.1 Hz), 69.71 (d, J = 138 Hz), 86.65, 172.89. ^{31}P NMR (162 MHz, $CDCl_3$, 25 °C) (δ, ppm): 25.67.

Polymerization of *n*-Butyl Acrylate with $DEPN_2$. $DEPN_2$ (106 mg, 0.134 mmol) and DEPN (17 mg, 0.057 mmol) were weighed into a 100 mL round-bottomed flask containing a magnetic stirbar. The flask was sealed with a three-way joint allowing introduction of reagents via syringe, application of vacuum, and nitrogen. The flask was evacuated to 60 mTorr and refilled with high-purity nitrogen three times. Purified *n*-butyl acrylate (25 mL, 174 mmol) was added and the mixture was degassed with three freeze−pump−thaw cycles. Finally, the flask was immersed in an oil bath thermostated at 130 °C for 75 min. After the polymerization, residual monomer was removed in vacuo (60 mTorr, 40 °C, 6 h). SEC analysis in THF revealed molecular weight data M_n = 23 700, M_w/M_n = 1.11.

Synthesis of Thymine-Containing Block Copolymer. Poly(*n*-butyl acrylate) homopolymer (5.15 g, M_n = 13 900) and 1-vinylbenzylthymine (1.46 g, 6.0 mmol) were added to a 50 mL round-bottomed flask with a magnetic stirbar. The flask was sealed with a three-way joint and evacuated to 60 mTorr and refilled with high-purity nitrogen three times. DMF (15 mL) was then syringed into the flask and the mixture was degassed with three freeze−pump−thaw cycles. The flask was then immersed in an oil bath at 120 °C for 5 h 40 min. After the polymerization, the polymer was isolated via precipitation into methanol. ^{1}H NMR spectroscopy ($CDCl_3$ +DMSO-d_6, 3:1 w/w) revealed block molecular weights $T_{1.8K}$-$nBA_{13.9K}$-$T_{1.8K}$. ^{1}H NMR (400 MHz, $CDCl_3$ + DMSO-d_6 (1:1 w/w), 25 °C) (δ, ppm): 0.86 (t, CH_3, 3H) 1.29 (q, $COOCH_2CH_2CH_2$-CH_3, 2H), 1.5 (br, C*H*$_2$−CH−COO and $COOCH_2CH_2$−), 1.7 (br, C*H*$_2$−CH−COO−, 1H), 2.1 (br, CH−COO-, 1H), 3.9 (br, $COOCH_2$, 2H), 4.7 (br, Ph−CH_2, 2H), 6.3 (br, Ph, 2H), 6.9 (br, Ph, 2H), 7.2 (br s, N−C═CH, 1H), 11.0 (s, NH, 1H).

Synthesis of Adenine-Containing Block Copolymer. Poly(*n*-butyl acrylate) homopolymer (4.83 g, M_n = 16 500) and 9-vinylbenzyladenine (0.99 g, 3.94 mmol) were added to a 50 mL round-bottomed flask with a magnetic stirbar. The flask was sealed with a three-way joint and evacuated to 60 mTorr and refilled with high-purity nitrogen three times. DMF (15 mL) was then syringed into the flask and the mixture was degassed with three freeze−pump−thaw cycles. The flask was then immersed in an oil bath at 122 °C for 5 h. After the polymerization, the polymer was isolated via precipitation into methanol. ^{1}H NMR spectroscopy revealed block molecular weights $A_{1.5K}$-$nBA_{16.5K}$-$A_{1.5K}$. ^{1}H NMR (400 MHz, DMSO-d_6, 25 °C) (δ, ppm): 0.86 (t, CH_3, 3H) 1.30 (q, $COOCH_2$-$CH_2CH_2CH_3$, 2H), 1.5 (br, C*H*$_2$−CH−COO and $COOCH_2$C*H*$_2$−), 1.75 (br, C*H*$_2$−CH−COO−, 1H), 2.2 (br, CH−COO−, 1H), 4.0 (br, $COOCH_2$, 2H), 5.2 (br, Ph−CH_2, 2H), 6.3 (br, Ph, 2H), 6.9 (br, Ph, 2H), 7.6 (br, NH_2, 2H), 8.1 (br, adenine ring protons, 2H).

Blends of Adenine and Thymine Functionalized Block Copolymers and Sample Preparation. An example of solution blending is provided for the A1 and T1 polymer set. Adenine-containing block copolymer $A_{1.5K}$-$nBA_{16.5K}$-$A_{1.5K}$ (0.300 g, 0.19 mmol A) and thymine-containing block copolymer $T_{1.8K}$-$nBA_{13.9K}$-$T_{1.8K}$ (0.216 g, 0.19 mmol T) were weighed into a vial containing a magnetic stirbar and chloroform (10 mL) was added. The vial was sealed and stirred for 18 h until the solid polymer was no longer visible. Films were cast in PTFE molds from solution and dried in a vacuum oven at 40 °C, with subsequent storage in a desiccator. Films were annealed at 155 °C under vacuum or 200 °C under nitrogen for 18 h.

For DMA and SAXS, polymer samples were cast from chloroform in PTFE molds and were dried under vacuum at 40 °C, with subsequent storage in a desiccator. In some cases (A1, T1, A1/T1), melt pressing (160 °C, 5 min) between PTFE films was necessary to obtain uniform films. Subsequent annealing steps were performed at 155 °C under vacuum for 18 h or at 135 °C under vacuum for A3, T3, and A3/T3. In some cases, annealing at 200 °C for 18 h was performed under nitrogen.

For AFM studies, polymer films were solution cast from chloroform (~0.5 wt % polymer) on silicon wafers at 3000 rpm, which resulted in thickness values near 100 nm. Prior cleaning of the silicon wafers consisted of rinsing with chloroform and drying under a high-pressure nitrogen stream. Annealing of the AFM film samples was conducted at 155 °C under vacuum or 200 °C under nitrogen for 18 h.

Polymer Characterization. In situ FTIR spectroscopic analysis was performed using a Mettler-Toledo ReactIR 1000 attenuated total reflectance (ATR) spectrometer equipped with a diamond composite (DiComp) probe.[50,51] Reaction kinetics were determined through the measuring the consumption of *n*-butyl acrylate, which was monitored with the disappearance of the acrylate absorbance at 968 cm^{-1}. Size exclusion chromatography (SEC) was performed at 40 °C in HPLC grade THF at 1 mL/min using a Waters size-exclusion chromatographer equipped with an autosampler, 3 in-line 5 μm PLgel MIXED-C columns. Detectors included a Waters 410 differential refractive index (DRI) detector operating at 880 nm, and a Wyatt Technologies miniDAWN multiangle 690 nm laser light scattering (MALLS) detector, calibrated with PS standards. All reported molecular weight values are absolute molecular weights obtained using the MALLS detector. ^{1}H NMR spectroscopic data

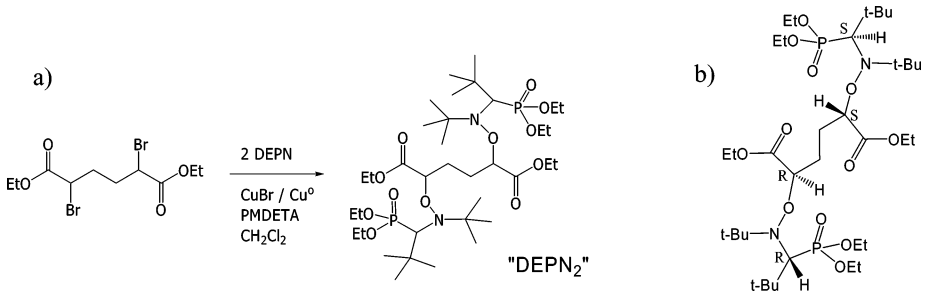

Figure 1. (a) Synthesis of $DEPN_2$, difunctional alkoxyamine initiator, using copper-promoted reaction of an activated dihalide. (b) Crystalline *meso* diastereomer of $DEPN_2$.

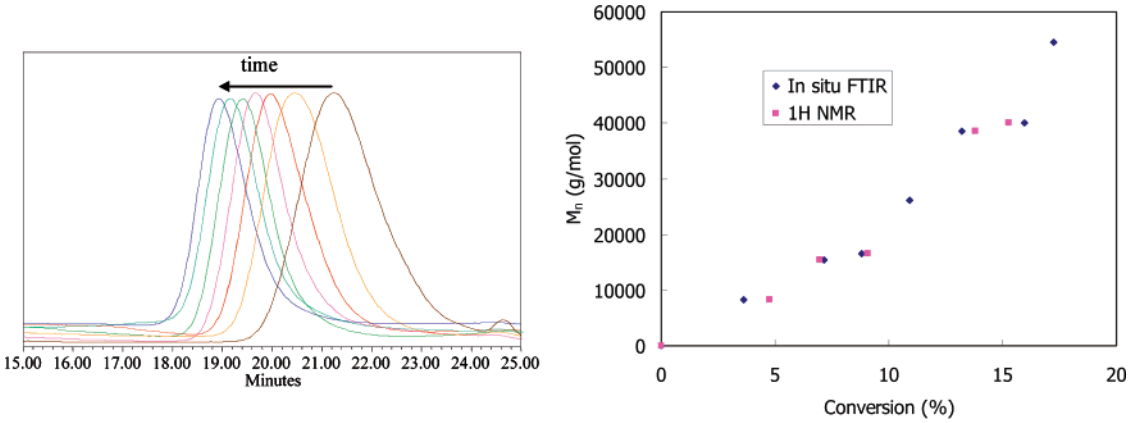

Figure 2. SEC analysis with time for the polymerization of *n*-butyl acrylate from $DEPN_2$ and linear molecular weight vs conversion plot.

was collected in $CDCl_3$ or mixtures of $CDCl_3$ and DMSO-d_6 and (3:1) on a Varian 400 MHz spectrometer at 25 °C. FAB MS was conducted in positive ion mode on a JEOL HX110 Dual Focusing mass spectrometer using xenon ion bombardment, poly(ethylene glycol) (PEG) standards and a 3-nitrobenzyl alcohol matrix.

DMA was conducted in film tension mode on 9.5 mm × 6.0 mm × 0.6 mm (l × w × t) rectangular strips on a TA Instruments Q800 DMA at a 3 °C/min scan rate, 1 Hz frequency. Solution rheology measurements were conducted on a TA Instruments G2 rheometer in concentric cylinder geometry in chloroform. Melt rheology was performed using a TA Instruments AR2000 rheometer at 1 Hz frequency and 2.5% strain at 160 °C.

A Veeco MultiMode scanning probe microscope was used for tapping-mode AFM imaging. Samples were imaged at a set-point ratio of 0.6 at magnifications of 500 nm × 500 nm. Veeco's Nanosensor silicon tips having spring constants of 10−130 N/m were utilized for imaging.

For small-angle X-ray (SAXS), Cu Kα X-ray radiation was generated using a Rigaku Ultrax18 rotating anode X-ray generator operated at 45 kV and 100 mA. A nickel filter was used to eliminate all wavelengths but the Cu Kα doublet, with an average wavelength of $\lambda = 1.542$ Å. The exact beam center and the sample-to-detector distance of approximately 1.5 m were calibrated using silver behenate.[52] The sample-to-detector distance was approximately 1.5 m. Two-dimensional data sets were collected using a Molecular Metrology 2D multiwire area detector, then corrected for detector noise, sample absorption, and background scattering. Azimuthal averaging of the corrected data, gave intensity as a function of the scattering vector, I(q), where $q = 4\pi \sin(\theta)/\lambda$ and 2θ is the scattering angle. The data were then placed on an absolute scale using a 1.07 mm thick type 2 glassy carbon sample, previously calibrated at the Advanced Photon Source in the Argonne National Laboratory, as a secondary standard. All data processing and analysis were done using Wavemetrics IGOR Pro 5.04 software and IGOR procedures written by Dr. Jan Ilavsky of Argonne National Laboratory.

Results and Discussion

Synthesis of a Novel Difunctional Alkoxyamine Initiator. A novel, difunctional alkoxyamine initiator based on DEPN ($DEPN_2$) was synthesized via conventional copper-promoted atom transfer radical addition techniques from a commercially available dihalide precursor (Figure 1).[53] $DEPN_2$ contains four chiral centers, which leads to the existence of 10 diastereomers, and typically an oily product. The chemical structure of $DEPN_2$ was confirmed via ^1H, ^{13}C and ^{31}P NMR spectroscopies as well as fast atom bombardment (FAB) mass spectrometry, however, the presence of multiple diastereomers complicated the spectral assignments. A *meso* diastereomer of $DEPN_2$ (RRSS, Figure 1) was isolated via chromatography in a crystalline form, and this was subjected to X-ray crystallography,[54] conclusively confirming the identity of the initiator. Unlike previously described difunctional alkoxyamine initiators,[45] $DEPN_2$ possesses a nonhydrolyzable linker in the main chain, which provides protection against hydrolytic degradation of the final polymer.

Performance of $DEPN_2$ in the Homopolymerization of *n*-Butyl Acrylate. The target nucleobase-containing block copolymers possess hydrogen-bonding styrenic outer blocks and a rubbery poly(*n*-butyl acrylate) central block (Figure 1). Thus, initial studies focused on evaluating the performance of $DEPN_2$ in *n*-butyl acrylate polymerization. Poly(*n*-butyl acrylate) offers a low glass transition temperature, which provides a wide service window for block copolymers ($T_g = -40$ °C).[55] Additional DEPN (0.4 equiv) was added to maintain control of the *n*-butyl acrylate polymerizations, which was shown previously to be necessary in the polymerization of acrylic monomers.[56]

In order to probe the performance of $DEPN_2$ in the homopolymerization of *n*-butyl acrylate, kinetic studies were coupled with absolute molecular weight determination using SEC analysis. In situ FTIR, which is a useful technique for monitoring

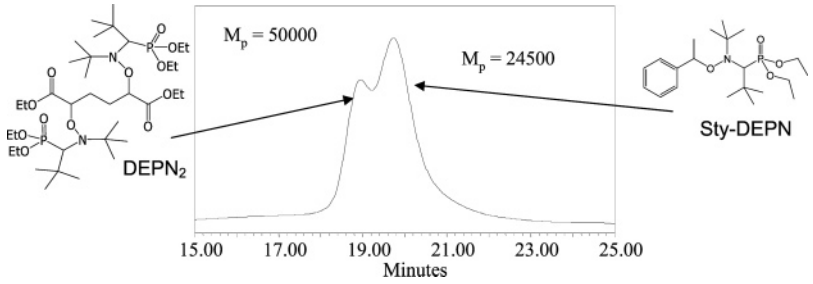

Figure 3. SEC trace from a polymerization containing DEPN$_2$ (difunctional) and Sty-DEPN[46] (monofunctional) initiators.

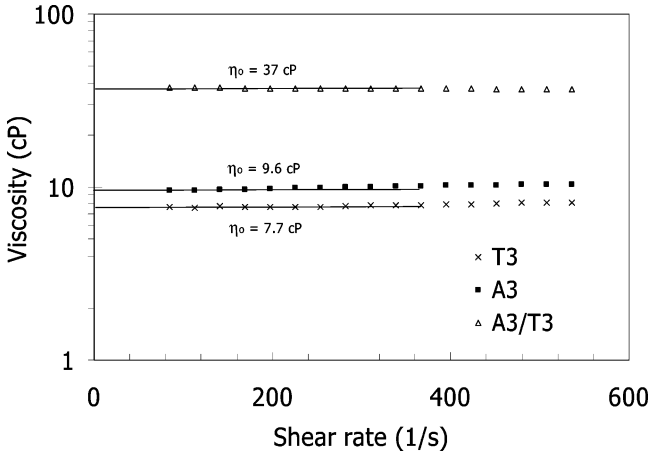

Figure 4. Solution rheology of hydrogen-bonding block copolymers (A3, T3 and their blend) in chloroform at 25 °C.

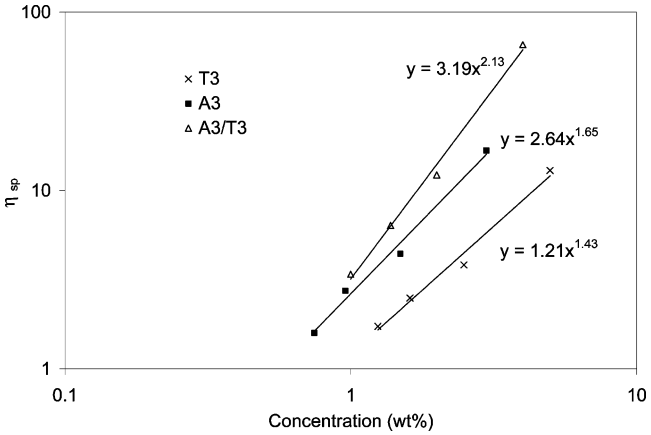

Figure 5. Zero-shear solution viscosities of the A3, T3 hydrogen-bonding block copolymers and their 1:1 A:T blend A3/T3 as a function of concentration.

reactions in real-time,[50] was employed to study the kinetics of the *n*-butyl acrylate homopolymerization through monitoring the disappearance of the acrylate absorbance at 968 cm^{-1} as previously reported.[44] The DEPN$_2$ initiated polymerizations of *n*-butyl acrylate exhibited *pseudo*-first-order kinetics, which was consistent with a controlled radical polymerization. SEC analysis of fractions that were removed from the reaction produced a linear molecular weight (M_n) vs conversion profile, which indicated a constant number of propagating chain ends that is consistent with a living polymerization process (Figure 2). Furthermore, SEC traces were unimodal with narrow polydispersities ($M_w/M_n \sim 1.10$), providing additional evidence for controlled radical polymerization.

Once the control of *n*-butyl acrylate polymerization with DEPN$_2$ was established, it was necessary to demonstrate the difunctional nature of DEPN$_2$, which is essential to the synthesis of well-defined triblock copolymers. This was accomplished using a technique that was developed in the earlier literature,[46] whereby *n*-butyl acrylate polymerizations were conducted with initiator mixtures of DEPN$_2$ and a monofunctional alkoxyamine initiator Sty-DEPN.[46] Assuming equal propagation rates for Sty-DEPN and the two initiating sites of DEPN$_2$, the molecular weight of the polymer formed with DEPN$_2$ should be higher (doubled compared to the Sty-DEPN initiated polymers). As shown in Figure 3, the SEC analysis of these polymers exhibited a bimodal molecular weight distribution with a 2:1 molecular weight ratio of the two peaks, which confirmed our assumption and the difunctional nature of DEPN$_2$.

Synthesis of Nucleobase-Functionalized Hydrogen-Bonding Block Copolymers. Initial efforts in the synthesis of block copolymers using DEPN$_2$ focused on optimizing the conditions for the synthesis of non-hydrogen-bonding poly(styrene-*b*-*n*-butyl acrylate-*b*-styrene) triblock copolymers. Block copolymerization, which was performed in a similar fashion to literature procedures,[45] was conducted in the absence of solvent at 120 °C without additional DEPN for the preparation of poly(styrene-*b*-*n*-butyl acrylate-*b*-styrene) triblock copolymers. Copolymerization reactions resulted in low polydispersities ($M_w/M_n = 1.17$) and unimodal SEC traces for a range of styrene block molecular weights (15K to 26K). Furthermore, optically clear, elastic block copolymer films were formed from solution casting, and AFM imaging revealed microphase-separated surface morphologies (Supporting Information).

Nucleobase-functionalized block copolymers were synthesized using analogous conditions to those for the synthesis of styrenic triblock copolymers. Adenine and thymine hydrogen-bonding groups were introduced via nucleobase-containing styrenic monomers, 1-vinylbenzylthymine and 9-vinylbenzyladenine (Scheme 1). In contrast to the bulk polymerizations of nonfunctional styrenic block copolymers, solvent (DMF) was employed to dissolve the solid nucleobase-containing monomers, which resulted in homogeneous polymerizations. Purified polymer products were obtained through precipitation into methanol, which removed residual monomers and solvent. ^{1}H NMR spectroscopy verified the presence of the nucleobases and quantified the degree of polymerization of the outer blocks, based on the SEC molecular weight of the poly(*n*-butyl acrylate) precursor block (Table 1; see Experimental Section for chemical shift values). Adenine-containing polymers with increasing poly(*n*-butyl acrylate) molecular weight were denoted as A1-A3, and thymine-containing polymers were denoted T1−T3. SEC analysis was also performed on the nucleobase-functionalized triblock copolymers in THF, which confirmed narrow molecular weight distributions and unimodal traces for the final triblock copolymers. However, SEC was not suitable for the determination of the number-average molecular weights of the hydrogen-bonding block due to the relatively short block lengths. Thus, ^{1}H NMR spectroscopy was used to calculate the molecular weights for the shorter hydrogen-bonding outer blocks. Blends of the complementary adenine- and thymine-containing poly-

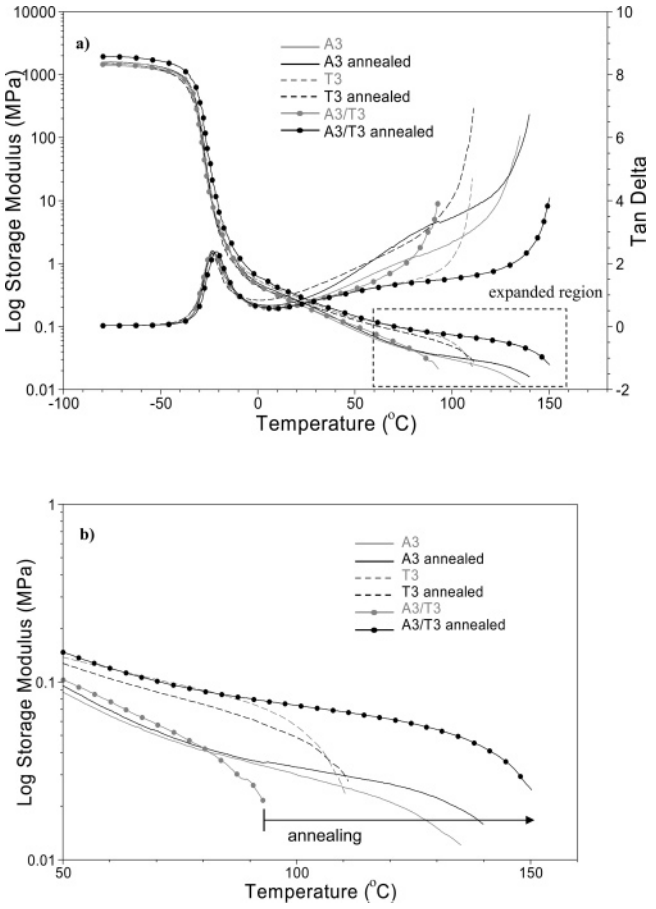

Figure 6. (a) Dynamic mechanical storage modulus and tan δ curves for adenine- and thymine-functionalized block copolymers A3, T3 and their blend A3/T3 (A:T = 1:1). Black lines represent samples that were annealed at 135 °C for 18 h under vacuum and gray lines represent unannealed samples. (b) Expansion of high-temperature softening. DMA conditions: film tension mode; 1 Hz; 3 °C/min; N_2.

mers of similar rubbery block molecular weights, denoted as A1/T1, A2/T2, and A3/T3, with a 1:1 ratio of adenine to thymine functional groups, were created via solution blending. These blends enabled investigations into the effects of complementary hydrogen bonding on the mechanical, rheological, thermal, and morphological properties of the triblock copolymers.

Complementary Hydrogen-Bonding Interactions in Solution and the Solid State. Hydrogen-bonding interactions in polymers typically manifest themselves in both the solid and solution state through changes in glass transition temperature, modulus, and viscosity. Hydrogen bond association constants (K_a) are commonly characterized in the solution state, using ^{1}H NMR[57] or FTIR[58] spectroscopy to examine changes in the chemical environment and bonding. These studies are typically performed in low dielectric constant solvents such as chloroform or toluene, in order to facilitate stronger hydrogen-bonding interactions while maintaining solubility of the polar heterocycles.[59] Our attempts to study complementary hydrogen bonding in the block copolymers using ^{1}H NMR spectroscopy were unsuccessful due to disappearance of the resonances for the hydrogen-bonding groups in spectra collected in low polarity solvents such as $CDCl_3$, presumably due to solution aggregation. This was particularly evident for the adenine-functionalized block copolymer (A2), where the nucleobase-functionalized blocks were visible in DMSO-d_6, but not in $CDCl_3$ (Supporting Information). ^{1}H NMR titration experiments of T3 with 9-octyladenine revealed expected chemical shift changes for the thymine NH (from 10.4 to 11.7 ppm upon addition of 2.1 equiv

Table 1. Molecular Weight Data for Nucleobase-Functionalized Block Copolymers and Blends

polymer	triblock mol wt	total mol wt (M_n)	precursor M_w/M_n[a]	wt % nucleobase monomer
A1	$A_{1.5K}$-nB$A_{16.5K}$-$A_{1.5K}$	19.5K	1.26	15
A2	$A_{2.8K}$-nB$A_{23.7K}$-$A_{2.8K}$	29.3K	1.11	19
A3	$A_{2.3K}$-nB$A_{62.3K}$-$A_{2.3K}$	66.9K	1.23	7
T1	$T_{1.8K}$-nB$A_{13.9K}$-$T_{1.8K}$	17.5K	1.23	21
T2	$T_{2.0K}$-nB$A_{23.7K}$-$T_{2.0K}$	27.7K	1.11	14
T3	$T_{1.4K}$-nB$A_{69.9K}$-$T_{1.4K}$	72.7K	1.22	4

[a] SEC: THF, 40 °C, MALLS

9-octyladenine). High solution viscosities and low concentrations of hydrogen-bonding groups also complicated FTIR analysis in solution.

Solution rheological experiments are often employed for the study of hydrogen-bonding systems, due to the sensitivity of viscosity to polymer structure in solution and the ability to tune the strength of hydrogen bonding through solvent polarity.[59−61] Solution rheological studies were performed on the hydrogen-bonding block copolymers in chloroform as a relatively low dielectric constant solvent. These studies were performed at a constant nucleobase concentration of 1.20 M, which led to different polymer concentrations among the samples due to slight differences in nucleobase block molecular weight. The presence of the complementary hydrogen-bonding interaction in solution was evident from the higher solution viscosities of the blend, which possessed an intermediate polymer concentration due to different nucleobase block molecular weights for the precursor polymers. The zero-shear viscosity of the blend was more than three times higher than the individual polymers (Figure 4), which suggested significant intermolecular hydrogen-bonding associations in solution. At the concentrations studied, the polymer solutions exhibited Newtonian behavior with the absence of shear thinning.

The zero-shear solution viscosity of the hydrogen-bonding triblock copolymers was also studied as a function of concentration in the semidilute unentangled regime.[62] In studying the concentration dependence of the zero-shear specific solution viscosity, different scaling exponents of the solution viscosities were observed compared to non-associating polymers. Typically, the zero-shear viscosity scales as $C^{1.25}$, for polymers below their entanglement concentration (C_e), while above C_e, viscosity scales as $C^{3.7}$ assuming that the polymer is dissolved in a good solvent.[63] As shown in Figure 5, the introduction of hydrogen-bonding groups led to scaling exponents of 1.4 and 1.6 for the thymine- and adenine-functionalized triblock copolymers respectively due to the weak self-association of the nucleobases ($K_{A-A} \sim K_{T-T} < 5\ M^{-1}$).[14] The blend of the two polymers led to the highest exponent of 2.1 and the greater slope as a function of hydrogen-bonding strength was presumed to result from the concentration dependence of the hydrogen-bonding equilibrium.[59] In the case of adenine and thymine hydrogen-bonding groups, neglecting self-association modes, the equilibrium can be written as

$$K_a = [AT]/[A][T] \quad (1)$$

where [A], [T], and [AT] are the concentrations of adenine, thymine and the associated complex of adenine and thymine and K_a is the association constant (130 M^{-1}).[14] Thus, as the concentration of the individual nucleobases increases, the concentration of the complex must increase to satisfy the equilibrium. In the case of hydrogen-bonding associations between polymers with multiple nucleobases, this leads to

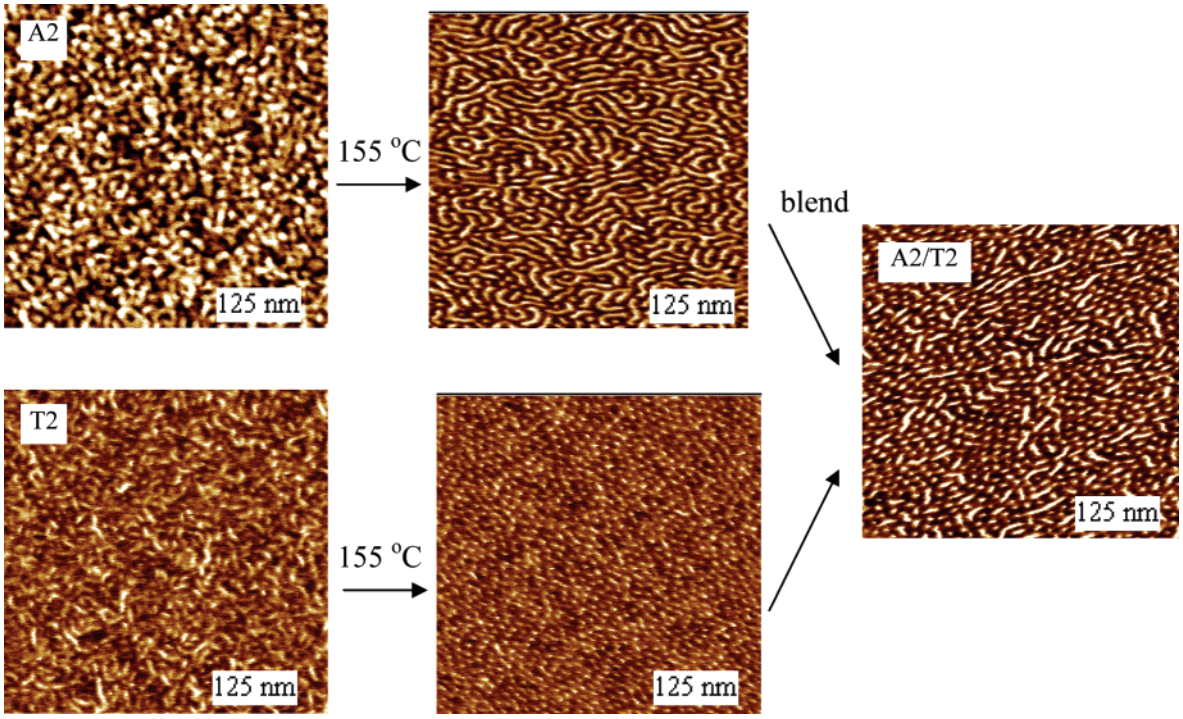

Figure 7. Tapping mode AFM phase images of thymine- (T2) and adenine-functionalized (A2) polymers before and after annealing as well as A2/T2 blend. Samples were spin-coated on a silicon wafer, from chloroform solution. Annealing was performed at 155 °C under vacuum for 18 h. Film thickness ~ 100 nm. Images are 500 nm × 500 nm.

Table 2. Small-angle X-ray Scattering Results for Hydrogen-bonding Block Copolymers

polymer	triblock mol wt	w_{Nu}[a] (%)	q^* (Å^{-1})	d (nm)	q_2 (Å^{-1})	q_3 (Å^{-1})	morphology[b]
A1	$A_{1.5K}$-n$BA_{16.5K}$-$A_{1.5K}$	15	0.042	15.0	0.072	0.112	Cyl
A2	$A_{2.8K}$-n$BA_{23.7K}$-$A_{2.8}$K	19	0.044	14.3			
A3	$T_{2.3K}$-n$BA_{62.3K}$-$T_{2.3K}$	7	0.029	21.7	0.052		Cyl
T1	$T_{1.8K}$-n$BA_{13.9K}$-$T_{1.8K}$	21	0.039	16.1	0.069	0.111	Cyl
T2	$T_{2.0K}$-n$BA_{23.7K}$-$T_{2.0K}$	14	0.052	12.1			
T3	$T_{1.4K}$-n$BA_{69.9K}$-$T_{1.4K}$	4	0.032	19.6	0.054		Cyl
A1/T1	N/A	18	0.040	15.7	0.074	0.121	Cyl
A2/T2	N/A	16	0.046	13.7			
A3/T3	N/A	6	0.033	19.0	0.058		Cyl

[a] Weight percent of nucleobase-functionalized block. [b] Assignments from SAXS maxima.

increased effective molecular weight of the supramolecular structures with increasing concentration. As Meijer has established, the formation of associated structures may be considered as a noncovalent step-growth process.[2] Since solution viscosity is a strong function of molecular weight, association is expected to lead to increased solution viscosity scaling exponents with concentration. Long et al. previously observed higher scaling exponents above C_e for PMMA which was randomly functionalized with ureidopyrimidone (UPy) quadruple hydrogen-bonding groups.[64]

Dynamic mechanical analysis (DMA) was utilized to examine the effects of hydrogen bonding on the thermomechanical behavior of the individual triblock copolymers as well as their complementary blends. Modulus vs temperature plots at a constant frequency (1 Hz) confirmed the multiphase nature of the block copolymers (A3 and T3, Figure 6). The soft block (poly(*n*-butyl acrylate)) glass transition temperature (T_g) occurred at −30 °C in each case whereas the hard block T_g occurred around 140 °C for the A3 and 110 °C for T3. This was consistent with measurements of the T_g of adenosine-functionalized methacrylate homopolymers synthesized by Haddleton et al., which possessed T_g values near 140 °C even for molecular weights below 10K.[34] A blend of the complementary adenine and thymine-containing polymers (A:T = 1:1 mole ratio), cast from solution, revealed a comparable softening temperature (140 °C). The absence of multiple softening transitions suggested the presence of a single hard phase consisting of mixed adenine- and thymine-containing polymer chains.

The samples were annealed at temperatures above the glass transitions (T_{anneal} = 135 °C), in order to obtain thermodynamically stable morphologies, that may be inaccessible due to strong hydrogen-bonding interactions at ambient temperature. Block copolymers typically require thermal annealing steps above the highest T_g, to develop an equilibrium morphology.[65−67] Due to strong intermolecular interactions, it was presumed that nucleobase-functionalized block copolymers would require annealing at higher temperatures. In DMA experiments, the individual adenine- and thymine-functionalized triblock copolymers did not exhibit significant change in their softening points upon annealing. In contrast with the individual triblock copolymers, the blend (A3/T3) exhibited a significant increase in the length of the rubbery plateau upon annealing, which extended to 150 °C. This was attributed to formation of an associated A−T hard phase that possessed greater thermomechanical integrity than the individual components, which exhibited relatively weaker self-complementary (A−A, T−T) hydrogen bonding. The presence of the associated hard phase was revealed with AFM studies (discussed in the following section) for the A2, T2, A2/T2 series.

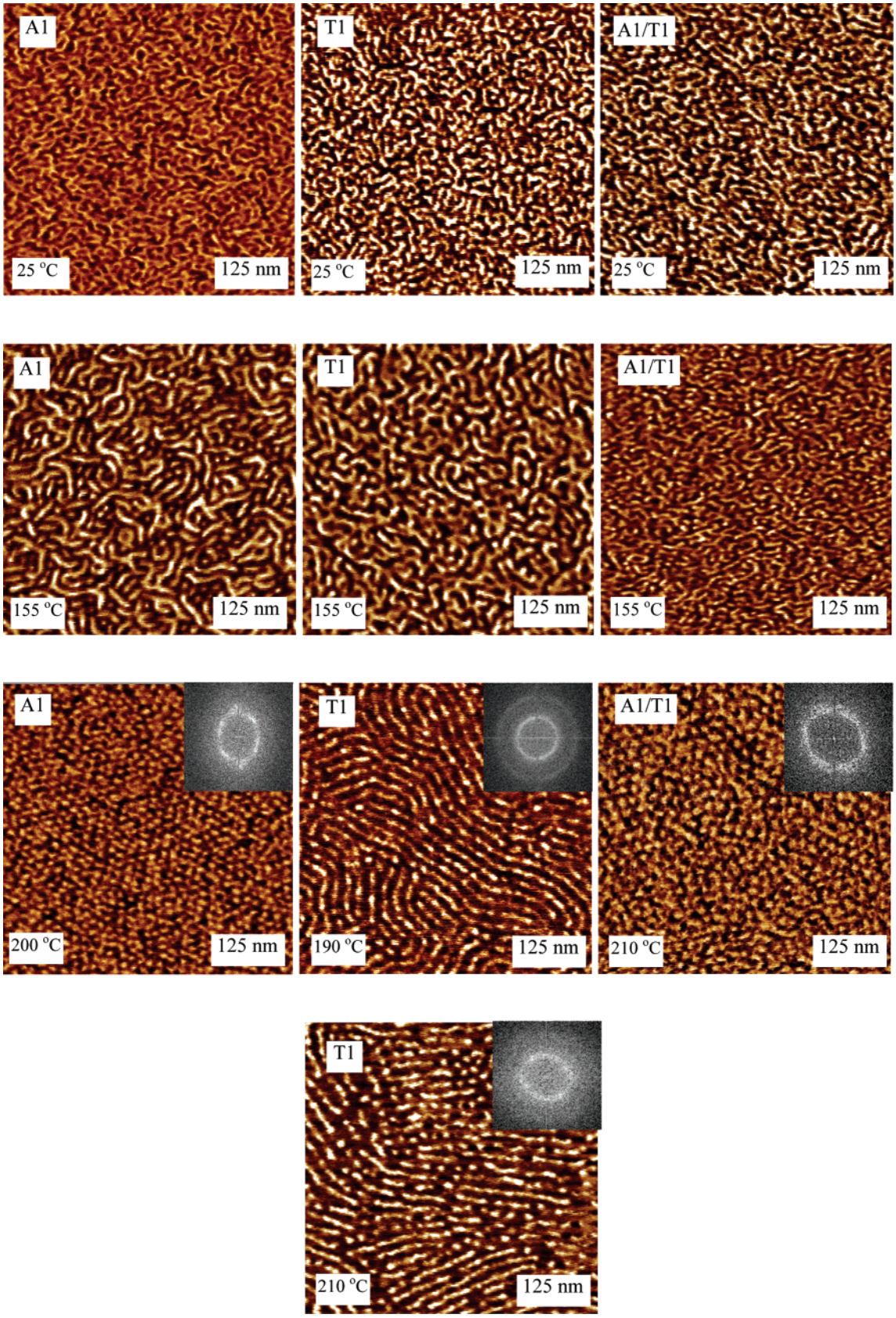

Figure 8. Tapping mode AFM phase images of A1, T1, and A1/T1 blend. Samples were spin- coated on silicon wafers, from chloroform solution. Annealing was performed at temperatures indicated in the lower left corners of each image, under vacuum for 18 h. Film thicknesses ~ 100 nm. Images are 500 nm × 500 nm. Set point ratio ~ 0.6. Insets are Fourier transforms (FFTs) of the phase images.

For samples containing higher hard block weight fractions (A1, T1), a longer rubbery plateau were observed (160 °C, not shown), and a similar, but less pronounced, enhancement in hard phase thermal integrity for the blend upon annealing was also observed. Storage modulus values at the rubbery plateau were also significantly higher (E'_{A1} = 0.6 MPa, E'_{T1} = 1.1 MPa, 80 °C) than those for the A3, T3 set due to the higher hard phase volume fraction.

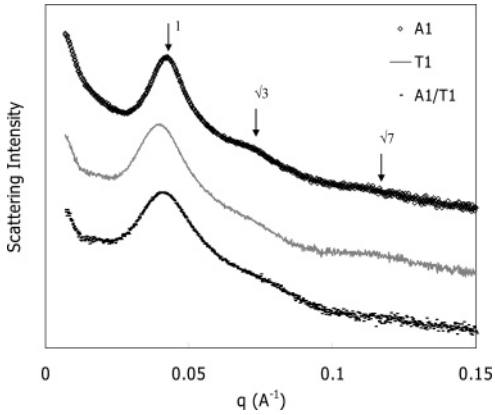

Figure 9. SAXS scattering profiles for nucleobase-containing polymers (A1, T1) and their 1:1 A:T blend. All samples annealed under vacuum at 155 °C for 18 h. Scattering maxima in terms of q/q^* are denoted with arrows.

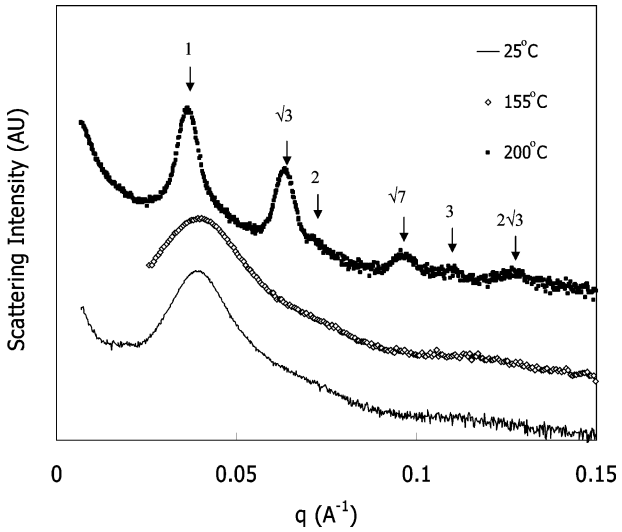

Figure 10. Effect of annealing conditions on thymine-containing triblock copolymer (T1) sample. Scattering maxima in terms of q/q^* are denoted with arrows.

Morphological Investigations of Nucleobase-Functionalized Block Copolymers and Blends. AFM allows imaging of surface texture and morphology of microphase-separated structures and is frequently applied to block copolymer films.[68,69] For both adenine- and thymine-containing polymers, AFM revealed intriguing surface morphologies, which consisted of hard domains of the nucleobase-functionalized styrene (light color) dispersed in a soft matrix of poly(*n*-butyl acrylate) (dark color) (Figure 7). Adenine- and thymine-functionalized block copolymers with identical rubber block molecular weights (A2 and T2), as well as their solution-cast equimolar nucleobase (1:1 A:T) blends, were spin-coated on silicon and imaged with AFM in tapping mode. Studies were conducted before and after annealing at 155 °C, which facilitated morphological development of the films. Unannealed samples exhibited microphase separation with generally poor shape development of domains and lack of ordering. Annealing produced distinct morphological features, with clear boundaries emerging between phases and development of short range order. Although AFM does not provide a definitive identification of bulk morphology, the thymine-containing block copolymer (T2) produced an apparent "end-on" cylindrical morphology (Figure 7). The presence of a cylindrical morphology was consistent with the moderate weight fraction of the outer blocks (14 wt %). The positioning of the hard domains appeared to indicate some degree of short-range

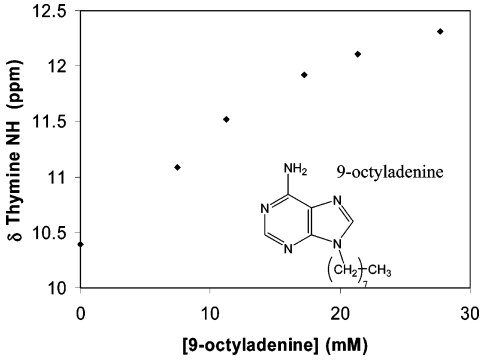

Figure 11. Chemical shift changes during introduction of 9-octyladenine to a thymine-containing triblock copolymer (T3).

hexagonally closest packed (hcp) order. AFM images of A2 resembled cylindrical morphologies where cylinders were lying in the plane of the image. Hobbs and Register observed similar images corresponding to cylindrical morphology in melts of poly(1,4-butadiene-*b*-3,4-isoprene).[68] Tsarkova et al. observed strikingly similar images of cylindrical morphologies of poly(styrene-*b*-butadiene) melts.[67] The blend of the two polymers (A2/T2) produced an intermediate morphology, presumably indicating the presence of cylinders lying both in the plane and perpendicular to the plane. The absence of macrophase separation in the blend suggested the compatibility of the complementary nucleobase functionalized hard blocks due to the hydrogen-bonding ability of the adenine and thymine blocks. This supposition was reinforced with SAXS analysis, having an averaged, intermediate Bragg spacing, and no evidence of multiple interdomain spacings, which is discussed in the following section. Furthermore, Choo et al. showed that thymine- and adenine-containing small molecules associate in the solid state into co-crystalline forms, upon simple grinding of a blend of the individual crystalline solids.[70]

Analogous AFM studies were conducted for the A1, T1, and A1/T1 set (Figure 8) which contained slightly higher nucleobase weight fractions (15−21 wt % for A1, T1, and A1/T1 vs 14−19 wt % for the A2, T2, and A2/T2 set) and slightly shorter rubber block molecular weights (13.9K or 15.9K vs 23.7K). As seen with the A2 and T2 series, the unannelaed samples exhibited poor morphological development. Annealing at 155 °C resulted in images that were similar to A2, resembling the "in plane" cylindrical morphology. Interestingly, the A1/T1 blend exhibited the least clear surface texture, possibly due to the strength of the complementary A−T hydrogen-bonding interactions preventing clear morphological development. The higher softening temperatures for the hard phases of T1 and T2 (160 °C), suggested that annealing at 155 °C was insufficient. In order to probe the effect of annealing at higher temperatures on block polymers containing the higher levels of nucleobases, annealing experiments were conducted on the A1, T1, and A1/T1 series at temperatures near 200 °C (Figure 8). Interestingly, annealing at temperatures near 200 °C enabled organization into "end-on" cylindrical morphologies for A1 and A1/T1 at the surface, and hcp ordering was observed as evidenced from the hexagonal shape of the Fourier transform of the AFM phase images. For the T1 sample, a well ordered cylindrical "in-plane" surface morphology was observed at 190 °C, followed by the beginning of a transition to "end-on" arrangement at 210 °C. SAXS experiments (discussed in the next section) conducted on the A1, T1 and A1/T1 set, annealed at 200 °C and 155 °C confirmed the cylindrical morphology in all cases. The hindered rearrangement of the thymine-containing polymer may have resulted from the fact that it possessed the highest nucleobase

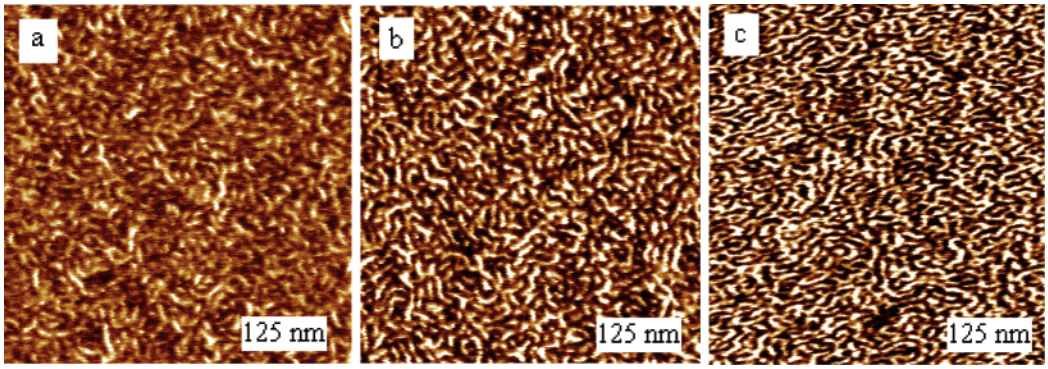

Figure 12. Tapping mode AFM images of unannealed thymine-functionalized block copolymer (T2) spin-coated on a silicon wafer from chloroform solutions containing (a) 0, (b) 0.4, and (c) 2.2 equiv of 9-octyladenine.

weight fraction (19 wt %) and lowest poly(*n*-butyl acrylate) block molecular weight (13.9K). Roose et al. also observed a transition upon annealing of "cylinders in the plane" to "end-on" cylinders for a poly(methyl methacrylate-*b*-methyl acrylate-*co*-ethylhexyl acrylate-*b*-methyl methacrylate).[65] The higher surface energy of the PMMA blocks was thought to result in the minimization of surface area of the hard domains, driving the system to the "end-on" morphology. In the present system, it is assumed that the polar nucleobase-containing blocks possess a higher surface energy than the poly(*n*-butyl acrylate) block, resulting in similar behavior.

While AFM was successful in characterizing the surface morphology of the block copolymers, SAXS enabled characterization of the larger scale bulk morphology of the nucleobase-functionalized block copolymers. SAXS experiments were conducted on individual adenine- and thymine-functionalized triblock copolymer as well as the corresponding 1:1 A:T blends. The presence of the Bragg diffraction maxima in the SAXS data confirmed the existence of microphase separation in all hydrogen-bonding triblock copolymers. The primary scattering maximum, centered at q^*, was used to determine the interdomain (Bragg) spacing present in each sample ($d = 2\pi/q^*$), listed in Table 2. The interdomain spacings measured with SAXS (12−20 nm) were similar to those observed with AFM. Additional secondary scattering maxima were observed in some cases, allowing morphological assignments. In the case of ∼15K poly(*n*-butyl acrylate) block samples (A1, T1), each individual polymer produced cylindrical morphology, as evidenced from the positions of the scattering maxima ($q/q^* = 1, \sqrt{3}, \sqrt{7}$)[71] (Figure 9). The expected maximum at $q/q^* = 2$ was not observed, but was believed to exist as a small shoulder on the peak at $q/q^* = \sqrt{3}$. The blend of the complementary block copolymers (A:T = 1:1) produced a similar cylindrical morphology with a Bragg spacing that was intermediate between the individual polymers. This trend of intermediate Bragg spacings for the blends was observed for the A2, T2 set as well and suggested the intimate mixing of the complementary hydrogen-bonding hard blocks producing an averaged interdomain spacing. For the ∼24K poly(*n*-butyl acrylate) block samples (A2, T2), secondary scattering peaks were not clearly resolved, which may be due to the casting conditions.(Supporting Information) The highest rubber block molecular weight samples (A3, T3) produced multiple scattering maxima, which were also attributed to cylindrical morphology.

Annealing studies with subsequent SAXS analysis were performed on the thymine-containing triblock copolymer with the highest nucleobase weight fraction (T1). As the annealing temperature increased, the scattering profile changed dramatically (Figure 10). Narrowing of the scattering maxima and the appearance of several readily discernible secondary maxima were observed. Annealing at 200 °C appeared to result in the clearest development of morphology in this sample, revealing scattering maxima of $q/q^* = 1, \sqrt{3}, 2, \sqrt{7}, 3$, and $2\sqrt{3}$, which corresponded to hexagonal closest packed (hcp) cylindrical morphology. Furthermore, the scattering maximum at $q/q^* = 2$ was observed as a clear shoulder on the maximum at $q/q^* = \sqrt{3}$. This suggested that elevated temperatures near 200 °C were necessary to achieve well-developed morphologies for the triblock copolymers with higher nucleobase weight fraction.

The adenine-containing triblock copolymer A1, and blend of adenine- and thymine-containing block copolymers (A1/T1) were also annealed at 200 °C, but did not exhibit the development of the order apparent in the T1 sample annealed at 200 °C. SAXS profiles of adenine-containing samples that were annealed at 200 °C resembled samples annealed at 155 °C. This may have resulted from possible cross-linking side reactions including nucleophilic attack of the adenine NH_2 to the *n*-butyl acrylate ester. In dynamic mechanical measurements, heating of the adenine-containing polymers above 200 °C resulted in cross-linking as evidenced from increasing storage modulus (E') and insolubility in solvents which previously dissolved the polymers. Melt rheological experiments at 150 and 160 °C indicated thermal stability at these reduced temperatures, and nearly constant shear storage modulus (G') and viscosity values were observed in the melt at 160 °C.

Introduction of Guest Molecules to Hydrogen-Bonding Block Copolymers. Hydrogen-bonding interactions facilitated the introduction of guest molecules containing complementary recognition units. Others have shown the recognition of guest molecules through hydrogen-bonding interactions in both solution[72] and the solid state.[73] Rotello et al. have used three-point hydrogen bonding between diacyldiaminopyridines and thymine to attach guest molecules containing flavin[3] or POSS to polystyrene.[73] Guest molecules also increase the solubility of hydrogen-bonding polymers through screening self-association of the polymer, thereby maintaining the homogeneity during polymerization reactions.[74]

A complementary alkylated adenine-containing small molecule guest (9-octyladenine, see Figure 12 for structure) was introduced into a thymine-containing block copolymer (T2 and T3). ^{1}H NMR titrations of T3 with 9-octyladenine indicated shifts in the peak position of the thymine NH proton to higher field (from 10.4 to 11.7 ppm) upon the addition of 2.2 equiv of 9-octyladenine (Figure 11). The curvature of the chemical shift data with increasing adenine concentration was consistent with typical NMR titration experiments in the literature.[57] Fitting this chemical shift data using the Benesi−Hildebrande method[57] produced an association constant of $K_a = 40\ M^{-1}$ and

demonstrated the noncovalent attachment of 9-octyladenine in the solution state. Unlike the association of the complementary triblock copolymers, where associations led to disappearance of the nucleobase resonances, the attachment of the guest molecule does not create restrictions on the motion of the polymer in solution, which makes ^{1}H NMR spectroscopic observation of the hydrogen-bonding interaction feasible.

For blends of 9-octyladenine with T2 in the solid state, AFM images indicated selective incorporation of the small molecule into the adenine-containing hard domains, as evidenced from increased phase contrast and greater hard phase continuity (Figure 12). Future efforts will be devoted to studying noncovalent attachment of other functionalities via hydrogen-bonding interactions.

Conclusions

Nucleobase-functionalized triblock copolymers with adenine- and thymine-containing outer blocks were synthesized for the first time via nitroxide mediated radical polymerization involving a novel difunctional initiator. Hydrogen-bonding interactions in blends of complementary polymers led to associations in solution that were manifested through dramatic increases in viscosity. Increased solution viscosity scaling exponents with concentration indicated the influence of the hydrogen-bonding equilibrium through increased effective molecular weight. In the solid state, hydrogen bonding led to compatibilization of the blends through the formation of an associated A−T hard phase. Morphological investigations of the individual block copolymers as well as their complementary blends revealed intermediate domain spacings and surface textures for blends of the complementary block copolymers. The introduction of complementary guest molecules resulted in selective uptake into nucleobase-containing domains which provides potential routes for drug delivery and biological applications.

Acknowledgment. The authors would like to thank Kraton Polymers for complementary funding and Dr. Carl Willis for insightful discussions. The authors would like to thank Askim F. Senyurt for helpful discussions during the writing of the manuscript. This material is based upon work supported by, or in part by, the U.S. Army Research Laboratory and the U.S. Army Research Office under Grant No. DAAD19-02-1-0275 Macromolecular Architecture for Performance (MAP) MURI.

Supporting Information Available: Text giving synthesis details for poly(styrene-*b*-*n*-butyl acrylate-*b*-styrene) from $DEPN_2$, and figures showing a reaction scheme, AFM images and SAXS data for A2, T2, and A2/T2, and ^{1}H NMR spectra. This material is available free of charge via the Internet at http://pubs.acs.org.

References and Notes

(1) Yamauchi, K.; Lizotte, J. R.; Hercules, D. M.; Vergne, M. J.; Long, T. E. *J. Am. Chem. Soc.* **2002**, *124*, 8599−8604.
(2) Brunsveld, L.; Folmer, B. J. B.; Meijer, E. W.; Sijbesma, R. P. *Chem. Rev.* **2001**, *101*, 4071−4098.
(3) Ilhan, F.; Galow, T. H.; Gray, M.; Clavier, G.; Rotello, V. M. *J. Am. Chem. Soc.* **2000**, *122*, 5895−5896.
(4) Lutz, J. F.; Thunemann, A. F.; Rurack, K. *Macromolecules* **2005**, *38*, 8124−8126.
(5) Deans, R.; Ilhan, F.; Rotello, V. M. *Macromolecules* **1999**, *32*, 4956−4960.
(6) Söntjens, S. H. M.; Sijbesma, R. P.; van Genderen, M. H. P.; Meijer, E. W. *J. Am. Chem. Soc.* **2000**, *122*, 7487−7493.
(7) Sotiropoulou, M.; Bokias, G.; Staikos, G. *Macromolecules* **2003**, *36*, 1349−1354.
(8) Yamauchi, K.; Kanomata, A.; Inoue, T.; Long, T. E. *Macromolecules* **2004**, *37*, 3519−3522.
(9) Beijer, F. H.; Sijbesma, R. P.; Kooijman, H.; Spek, A. L.; Meijer, E. W. *J. Am. Chem. Soc.* **1998**, *120*, 6761−6769.
(10) Beijer, F. H.; Sijbesma, R. P.; Vekemans, J. A. J. M.; Meijer, E. W. K. H.; Spek, A. L. *J. Org. Chem.* **1996**, *61*, 6371−6380.
(11) Jorgensen, W. L.; Pranata, J. *J. Am. Chem. Soc.* **1990**, *112*, 2008−2010.
(12) Pranata, J.; Wierschke, S. G.; Jorgensen, W. L. *J. Am. Chem. Soc.* **1991**, *113*, 2810−2819.
(13) Roland, J. T.; Guan, Z. *J. Am. Chem. Soc.* **2004**, *126*, 14328−14329.
(14) Kyogoku, Y.; Lord, R. C.; Rich, A. *Proc Natl Acad Sci U.S.A.* **1967**, *57*, 250−257.
(15) Guan, Z.; Roland, J. T.; Bai, J. Z.; Ma, S. X.; McIntire, T. M.; Nguyen, M. *J. Am. Chem. Soc.* **2004**, *126*, 2058−2065.
(16) Sivakova, S.; Rowan, S. J. *Chem. Soc. Rev.* **2005**, *34*, 9−21.
(17) Sivakova, S.; Bohnsak, D. A.; Mackay, M. E.; Suwanmala, P.; Rowan, S. J. *J. Am. Chem. Soc.* **2005**, *127*, 18202−18211.
(18) Ghosal, G.; Muniyappa, K. *Biochem. Biophys. Res. Comm* **2006**, *343*, 1−7.
(19) Pan, J.; Chen, M.; Warner, W.; He, M.; Dalton, L.; Hogen-Esch, T. E. *Macromolecules* **2000**, *33*, 7835−7841.
(20) Kriz, J.; Dybal, J.; Brus, J. *J. Phys. Chem. B* **2006**, *110*, 18338−18346.
(21) Klinedinst, D. B.; Yilgor, E.; Yilgor, I.; Beyer, F. L.; Sheth, J. P.; Wilkes, G. L. *Rubber Chem. Technol.* **2005**, *78*, 737−753.
(22) Leibler, L. *Macromolecules* **1980**, *13*, 1602−1617.
(23) Lee, K. M.; Han, C. D. *Macromolecules* **2002**, *35*, 3145−3156.
(24) Nowick, J. S.; Chen, J. S.; Noronha, G. *J. Am. Chem. Soc.* **1993**, *115*, 7636−7644.
(25) Spijker, H. J.; Dirks, A. J.; van Hest, J. C. M. *Polymer* **2005**, *46*, 8528−8535.
(26) Zhou, J.; Li, Z.; Liu, G. *Macromolecules* **2002**, *35*, 3690−3696.
(27) Liu, G.; Zhou, J. *Macromolecules* **2003**, *36*, 5279−5284.
(28) Hu, J.; Lui, G. *Macromolecules* **2005**, *38*, 8058−8065.
(29) Yan, X.; Liu, G.; Hu, J.; Willson, C. G. *Macromolecules* **2006**, *39*, 1906−1912.
(30) Li, Z.; Ding, J.; Day, M.; Tao, Y. *Macromolecules* **2006**, *39*, 2629−2636.
(31) Bazzi, H.; Sleiman, H. *Macromolecules* **2002**, *35*, 9617−9620.
(32) Nair, K. P.; Pollino, J. M.; Weck, M. *Macromolecules* **2006**, *39*, 931−940.
(33) Noro, A.; Nagata, Y.; Tsukamoto, M.; Hayakawa, Y.; Takano, A.; Matsushita, Y. *Biomacromolecules* **2005**, *6*, 2328−2333.
(34) Marsh, A.; Khan, A.; Haddleton, D. H.; Hannon, M. J. *Macromolecules* **1999**, *32*, 8725−8731.
(35) Lutz, J. F.; Thunemann, A. F.; Nehring, R. *J. Polym. Sci., Part A: Polym. Chem.* **2005**, *43*, 4805−4818.
(36) Puskas, J. E.; Dahman, Y.; Margaritas, A.; Cunningham, M. F. *Biomacromolecules* **2004**, *5*, 1412−1421.
(37) Brahme, N. M.; Smith, W. T. *J. Polym. Sci., Part A: Polym. Chem.* **1984**, *22*, 813−820.
(38) Kaye, H. *Macromolecules* **1971**, *4*, 147−152.
(39) Inaki, Y. *Prog. Polym. Sci.* **1992**, *17*, 515−570.
(40) Hawker, C. J.; Bosman, A. W.; Harth, E. *Chem. Rev.* **2001**, *101*, 3661−3688.
(41) Saito, K.; Ingalls, L.; Warner, J. C. *Polym Prep* **2006**, *47*, 829−830.
(42) Grimaldi, S.; Finet, J. P.; Le Moigne, F.; Zeghdaoui, A.; Tordo, P.; Benoit, D.; Fontanille, M.; Gnanou, Y. *Macromolecules* **2000**, *33*, 1141−1147.
(43) Robin, S.; Gnanou, Y. *Macromol. Symp.* **2001**, *165*, 43−53.
(44) Mather, B. D.; Lizotte, J. R.; Long, T. E. *Macromolecules* **2004**, *37*, 9331−9337.
(45) Robin, S.; Guerret, O.; Couturier, J. L.; Pirri, R.; Gnanou, Y. *Macromolecules* **2002**, *35*, 3844−3848.
(46) Diaz, T.; Fischer, A.; Jonquieres, A.; Brembilla, A.; Lochon, P. *Macromolecules* **2003**, *36*, 2235−2241.
(47) Sedlak, M.; Simunek, P.; Antonietti, M. *J. Heterocyclic Chem.* **2003**, *40*, 671−675.
(48) Srivatsan, S. G.; Parvez, M.; Verma, S. *Chem.—Eur. J.* **2002**, *8*, 5184−5191.
(49) Bunton, C. A.; Wolfe, B. B. *J. Am. Chem. Soc.* **1974**, *96*, 7747−7752.
(50) Pasquale, A. J.; Lizotte, J. R.; Williamson, D. T.; Long, T. E. *Polym News* **2002**, *27*, 272−283.
(51) Lizotte, J. R.; Long, T. E. *Macromol. Chem. Phys.* **2003**, *204*, 570−576.
(52) Huang, T. C.; Toraya, H.; Blanton, T. N.; Wu, Y. *J. Appl. Crystallogr.* **1993**, *26*, 180−184.
(53) Matyjaszewski, K.; Woodworth, B. E.; Zhang, X.; Gaynor, S.; Metzner, Z. *Macromolecules* **1998**, *31*, 5955−5957.
(54) Mather, B. D.; Baker, M. B.; Beyer, F. L.; Green, M. D.; Berg, M. A. G.; Long, T. E. *Macromolecules* **2007**, *40*, 4396−4398.
(55) Brandrup, J.; Immergut, E. H. *Polymer Handbook*, 3rd ed.; Wiley: New York, 1989.

(56) Lacroix-Desmazes, P.; Lutz, J. F.; Chauvin, F.; Severac, R.; Boutevin, B. *Macromolecules* **2001**, *34*, 8866−8871.
(57) Fielding, L. *Tetrahedron* **2000**, *56*, 6151−6170.
(58) Kyogoku, Y.; Lord, R. C.; Rich, A. *J. Am. Chem. Soc.* **1967**, *89*, 496−504.
(59) Sijbesma, R. P.; Beijer, F. H.; Brunsveld, L.; Folmer, B. J. B.; Hirschberg, J. H. K. K.; Lange, R. F. M.; Lowe, J. K. L.; Meijer, E. W. *Science* **1997**, *278*, 1601−1604.
(60) Karikari, A.; Mather, B. D.; Long, T. E. *Biomacromolecules* **2007**, *8*, 302−308.
(61) Lange, R. F. M.; van Gurp, M.; Meijer, E. W. *J. Polym. Sci., Part A: Polym. Chem.* **1999**, *37*, 3657−3670.
(62) de Gennes, P. G. *Scaling Concepts in Polymer Physics*; Cornell University: Ithaca, NY, 1979.
(63) Colby, R. H.; Rubinstein, M. *Macromolecules* **1990**, *23*, 2753−2757.
(64) McKee, M. G.; Elkins, C.; Long, T. E. *Polymer* **2004**, *45*, 8705−8715.
(65) Jeusette, M.; Leclere, P.; Lazzaroni, R.; Simal, F.; Vaneecke, J.; Lardot, T.; Roose, P. *Macromolecules* **2007**, *40*, 1055−1065.
(66) Marcos, A. G.; Pusel, T. M.; Thomann, R.; Pakula, T.; Okrasa, L.; Geppert, S.; Gronski, W.; Frey, H. *Macromolecules* **2006**, *39*, 971−977.
(67) Tsarkova, L.; Horvat, A.; Krausch, G.; Zvelindovsky, A. V.; Sevink, G. J. A.; Magerle, R. *Langmuir* **2006**, *22*, 8089−8095.
(68) Hobbs, J. N.; Register, R. A. *Macromolecules* **2006**, *39*, 703−710.
(69) Ott, H.; Abetz, V.; Altstadt, V.; Thomann, Y.; Pfau, A. *J. Microsc.* **2002**, *205*, 106−108.
(70) Etter, M. C.; Reutzel, S. M.; Choo, C. G. *J. Am. Chem. Soc.* **1993**, *115*, 4411−4412.
(71) Mani, S.; Weiss, R. A.; Hahn, S. F.; Williams, C. E.; Cantino, M. E.; Khairallah, L. H. *Polymer* **1998**, *10*, 2023−2033.
(72) Thibault, R. J.; Hotchkiss, P. J.; Gray, M.; Rotello, V. M. *J. Am. Chem. Soc.* **2003**, *125*, 11249−11252.
(73) Carroll, J. B.; Waddon, A. J.; Nakade, H.; Rotello, V. M. *Macromolecules* **2003**, *36*, 6289−6291.
(74) Stubbs, L. P.; Weck, M. *Chem.−Eur. J.* **2003**, *9*, 992−999.

MA070865Y